TECHNICAL REPORT

A METHOD FOR DETERMINING CATALYTIC EFFICIENCY OF SURFACES

By: I. O. Bohachevsky and D. F. DeSanto

CAL No. AI-2187-A-4

Prepared under the following:

NASA Contract NAS 5-9978
NASA Contract NAS 5-3976
AFOSR Contract AF 49(630)-1487
CAL W/A 7152-146

FEBRUARY 1967

CORNELL AERONAUTICAL LABORATORY, INC.

OF CORNELL UNIVERSITY, BUFFALO, N. Y. 14221

CORNELL AERONAUTICAL LABORATORY, INC.
BUFFALO, NEW YORK 14221

A METHOD FOR DETERMINING CATALYTIC EFFICIENCY OF SURFACES

CAL REPORT NO. AI-2187-A-4

Prepared under the following:

NASA Contract NAS 5-9978
NASA Contract NAS 5-3976
AFOSR Contract [redacted] AF 49(638)1487
CAL W/A 7152-146

AF 49(638)-1487

FEBRUARY 1967

PREPARED BY: I.O. Bohachevsky

I.O. Bohachevsky
Aerodynamic Research Department

APPROVED BY: J. Gordon Hall

J. Gordon Hall, Head
Aerodynamic Research Department

D.F. DeSanto

D.F. DeSanto
Applied Mechanics Department

FOREWORD

The work described in this report was supported in part by the National Aeronautics and Space Administration, Goddard Space Flight Center under Contracts NAS 5-9978 and NAS 5-3976, in part by the Air Force Office of Scientific Research of the Office of Aerospace Research under Contract AF 49(638)-1487, and in part by CAL internal funds on Work Authorization 7152-146.

The authors are grateful to Dr. A. L. Myerson, who suggested the problem and supplied a large amount of necessary background information. They are also indebted to Dr. M. G. Dunn, Dr. S-W. Kang, and Dr. C. E. Treanor for helpful suggestions in the preparation of the manuscript. The programming and computations were ably carried out by Mr. J. R. Moselle; without his competent and enthusiastic cooperation this work would not have been possible.

ABSTRACT

A method is described which is used to determine numerically the relationship between the catalytic efficiency (γ) of a surface and the heat transfer ($\dot{q}$) through the surface in low Reynolds number flow of a partially dissociated gas. The work is motivated by the fact that heat transfer is easily measurable in the laboratory whereas catalytic efficiency is not. The approach is directed towards the derivation of a relationship between γ and the surface concentration of free atoms (c_o); once this relationship is known, it is used to eliminate c_o from the expression relating γ and $\dot{q}$, obtainable from energy balance and from the kinetic theory of gases. To establish the required relationship between γ and c_o , a mixed boundary value problem for the convective diffusion equation is formulated and solved numerically using an implicit, alternating-direction iteration procedure. The concentration of free atoms is determined not only along the surface, but also throughout the flow field. Results are obtained for a cylinder partially coated with a catalytic substance; they reveal the effect of the velocity field and point out the need for better quantitative knowledge of the low Reynolds number flow. In addition, parameter values for the best experimental accuracy are delineated.

TABLE OF CONTENTS

LIST OF SYMBOLS

a	Cylinder radius, cm
c	Atomic species concentration (mole fraction of free atoms)
D	Binary diffusion coefficient, cm^2/sec
ΔH	Heat of dissociation of diatomic gas, cal/mole
j	Index of radial coordinate
$\bar{J}$	Maximum value of j (positive integer)
m	Index of angular coordinate
$\bar{M}$	Maximum value of m (positive integer)
M	Molecular weight of diatomic species, gram/mole
n	Number of iteration cycle (positive integer)
p_t	Total gas pressure, $dyne/cm^2$ or mm Hg
$\dot{q}$	Heat flux through cylinder surface, cal/cm^2-sec
R_o	Universal gas constant, $= 8.314 \times 10^7$ erg/mole-°K
Re	Reynolds number, $U_\infty a/\bar{\nu}$
T	Temperature, °K
u	Dimensionless radial velocity component
U_∞	Free-stream velocity, cm/sec
v	Dimensionless tangential velocity component
γ	Catalytic efficiency of surface
Γ	Euler's constant, 0.577...
θ	Angular coordinate, deg or rad
$\Delta\theta$	Increment in angular coordinate, deg or rad

θ_c	Angular extent of catalytic portion of cylinder surface (see Fig. 1), deg or rad
κ	Overrelaxation parameter in iteration scheme (see Eq. (AI-2))
λ	$-D\left(\pi M/R_o T\right)^{1/2}/a\gamma$
ν	Dimensionless diffusivity $D/U_\infty a$
$\bar{\nu}$	Kinematic viscosity, cm^2/sec
ρ	Dimensionless radial coordinate
$\Delta\rho$	Increment in dimensionless radial coordinate

Subscripts

o	At cylinder surface
∞	Remote from cylinder

Other symbols defined in text.

LIST OF ILLUSTRATIONS

INTRODUCTION

Study of the catalytic effects of solid surfaces is desirable in order to gain basic understanding of heterogeneous physicochemical phenomena. It is expected that such understanding will assist in the determination of the reaction rates for certain recombination processes. This knowledge may be of considerable practical importance in connection with the problem of heat transfer to aerospace vehicles: in the case of maneuverable reentry vehicles which will spend considerable time in the atmosphere, the heat released by the recombination of dissociated gas atoms may be a significant (if not dominant) fraction of the total heat load experienced during reentry.

The heat shields used to protect the spacecraft from aerodynamic heating are, in general, constructed from materials which react with the surrounding air and thus contribute various chemical species that diffuse through the velocity field surrounding the vehicle. The study of the distribution of these species, in particular ions and electrons, is important in connection with the problem of communication through the plasma sheath which envelops the reentry vehicle. The method of solution developed in Sec. II of this paper may be used to obtain a considerable amount of information about the species distribution.

Because of the aforementioned reasons, the problem treated in this paper has recently received considerable attention, both theoretical and experimental. In particular, it has been pointed out[1] that the effects of convective and diffusive velocities may affect the reaction rate very strongly.

In the present approach we assume that the velocity field through which diffusion occurs is specified beforehand, i. e., is decoupled from the diffusion process. Our original intention was to carry out calculations for Oseen flow around a cylinder; however, the existing explicit analytic solution of the Oseen equations[2] turned out to be unsuitable for numerical application. Therefore, the investigation was carried out for several

velocity fields which hopefully approximate the low Reynolds number flow near a circular cylinder. These approximations are described in Sec. II. 3, and the effect of varying the velocity field is examined in the discussion of the results.

I. GENERAL PROCEDURE

We base our considerations on the assumption that there exists a unique relationship (for given flight or experimental conditions) between the catalytic efficiency, γ, of the surface and the heat flux, $\dot{q}$, through the surface. (By γ we shall mean the fraction of collisions between free atoms and the surface which result in atom recombination.) It is clear from physical arguments that if all other parameters of the process remain unchanged and if the velocity field is uncoupled from chemical effects, such a functional dependence should exist. The question, therefore, is how to find it.

Using the definition of γ, together with consideration from the kinetic theory of gases, Prok[3] has derived the following relationship which holds under the assumption that all of the heat generated by the recombination process enters the surface:*

$$\gamma = \frac{2\dot{q}\, M/\Delta H}{p_t\, c_o \sqrt{\frac{M}{\pi R_o T}} + \dot{q}\, M/\Delta H} \qquad (1)$$

where p_t is the total pressure in dynes/cm^2, M is the molecular weight of the diatomic gas, $R_o = 8.314 \times 10^7$ erg/mole/°K is the universal gas constant, T is the temperature in °K, $\dot{q}$ is measured in cal/cm^2/sec., and ΔH is the heat of dissociation of the diatomic gas in cal/mole. Unfortunately, this expression contains the mole fraction c_o of free atoms at the surface which, in general, is unknown.

In the present investigation, heat transfer rates (Figs. 6-9) have been computed using Eq. (1). Assuming a first-order recombination reaction at the surface (Eq.(3d)) and employing the equation of state for the gas mixture and the definition of the diffusion coefficient, it is possible to derive the following relation involving γ, $\dot{q}$, and c_o which is slightly different from Eq. (1):

$$\gamma = \frac{2\dot{q}\, M/\Delta H}{p_t\, c_o \sqrt{\frac{M}{\pi R_o T}}}$$

The latter equation is strictly consistent with the boundary condition and other basic relations mentioned previously, whereas Prok's equation, Eq. (1), is not (except in the limit for vanishingly small γ). The difference in heat transfer rate associated with using the two different equations is relatively small for the range of values of catalytic efficiency considered in this study, varying from zero at $\gamma = 0$ to a maximum of 10 percent at $\gamma = 0.2$.

If, however, we assume a definite value for γ, then we can calculate the corresponding surface concentration c_o by solving a mixed boundary value problem for the diffusion equation with convective terms present. Performing such calculations for various values of γ, we obtain for each point on the surface a graph of c_o versus γ. This means that we will know the pairs of corresponding values of γ and c_o and, therefore, will be able to use Eq. (1) for plotting the relationship between $\dot{q}$ and γ from which c_o has been eliminated.

We now proceed with the description of the method used to determine the surface concentration as a function of γ.

II. CONVECTIVE DIFFUSION IN THE PRESENCE OF A CATALYTIC SURFACE

1. Formulation of the Problem

The nature of the mathematical problem requires that a solution be obtained for the concentration throughout the flow field. The desired surface concentration then consists of the value that this solution takes on at the inner boundary.

To facilitate the presentation of the method for determination of the concentration field, we assume a specific situation, depicted in Fig. 1: a low-velocity, plane flow of diatomic molecules carries a given mole fraction c_∞ of dissociated free atoms around a cylinder whose front portion is covered by a catalytic material; the remainder of the cylinder surface is noncatalytic. This configuration represents a common experimental arrangement.

The steady-state diffusion of atoms through the resulting flow field is governed by the convective diffusion equation, which, in polar coordinates is:

$$u \frac{\partial c}{\partial \rho} + \frac{1}{\rho} v \frac{\partial c}{\partial \theta} = \nu \nabla^2 c \qquad (2)$$

where u and v are the radial and tangential velocity components, respectively, made nondimensional with respect to the free-stream velocity at infinity, U_∞, the radius ρ is made nondimensional with respect to the cylinder radius a, and ν is the nondimensional diffusivity $D/U_\infty a$ (the reciprocal of the diffusion Reynolds number), D being the binary diffusion coefficient at the given pressure and temperature. The velocity components u and v are assumed known (see Sec. II. 3).

Equation (2) is supplemented with the following boundary conditions:

$$
\begin{aligned}
&\text{(a).}\quad c \longrightarrow c_\infty \ \text{ as } \ \rho \longrightarrow \infty && \pi \geq \theta \geq \frac{\pi}{2} \\
&\text{(b).}\quad u\frac{\partial c}{\partial \rho} + \frac{1}{\rho} v \frac{\partial c}{\partial \theta} \longrightarrow 0 \ \text{ as } \ \rho \longrightarrow \infty && \frac{\pi}{2} > \theta \geq 0 \\
&\text{(c).}\quad \frac{\partial c}{\partial \rho} = 0 \ \text{ at } \ \rho = 1 && 0 \leq \theta \leq \theta_c \\
&\text{(d).}\quad c + \lambda \frac{\partial c}{\partial \rho} = 0 \ \text{ at } \ \rho = 1 && \theta_c \leq \theta \leq \pi
\end{aligned}
\qquad (3)
$$

Condition (b) was selected in preference to the simpler condition $c \longrightarrow c_\infty$ in order to account for any downstream reduction in free atom concentration associated with surface recombination. Condition (d) with $\lambda = -D(\pi M/R_o T)^{1/2}/a\gamma$ is easily shown to represent a first-order reaction at the surface. The angle θ_c defining the extent of the catalytic portion of the cylinder surface can have any value between 0 and π .

2. Method of Solution

2.1 Finite-difference formulation

The differential problem formulated in the previous section has been solved by a finite-difference technique, whereby the derivative terms in the governing differential equation and in the boundary conditions are replaced by divided differences at discrete points ("mesh points") distributed on a lattice which extends over the flow field. The resulting set of simultaneous algebraic equations is then solved numerically. Because the problem is a boundary value problem with boundaries at the body surface and also remote from the body, the numerical procedure must be iterative.

2.2 Selection of iteration scheme

Many possible iteration schemes for solving the simultaneous finite-difference equations corresponding to Eq. (2) and its boundary conditions can be set forth. Here we shall distinguish two general types of iteration scheme: explicit and implicit. In both methods, an initial guess is made of the value of the solution at every mesh point, following which a measure of the error associated with the guess is computed at each point. (The error at a point is taken to be the amount by which the finite-difference

analog of the governing differential equation, Eq. (2), fails to be satisfied at that point; this is called the residue.) In explicit schemes, the guess is changed at each mesh point by an amount proportional to the residue at the point; new residues are then computed and new iterates formed until every residue is reduced to an acceptably small value. In implicit schemes, on the other hand, a linear combination of values at specified adjacent mesh points is changed in each iteration cycle, rather than the value at a single point. It is evident that implicit schemes are more complicated than explicit ones; however, the additional complexities involved are more than compensated by the shortening of the overall computation time needed to achieve convergence. This is true because relatively large changes in successive iterates can be made in implicit schemes, whereas only small changes can be made in explicit schemes--otherwise the solution will diverge. For the present problem, the error between the initial guess and the true solution can be reduced only by a factor of $(\Delta\rho)^2/100$ per iteration cycle, using an explicit scheme (see Appendix I), whereas the implicit scheme described and analyzed in Appendix II is, for all practical purposes, unconditionally convergent and therefore requires thousands of times fewer cycles to approach the correct value of the solution. Consequently, the latter has been used in our work.

2.3 Numerical solution procedure

The implicit iteration scheme that has been selected for the present problem is an alternating-direction type,[4] consisting of solving successively the following two equations which constitute a finite-difference analog of Eq. (2) (see Appendix II for details):

$$k\left[\frac{\nu}{(\Delta\rho)^2}+\frac{1}{2\Delta\rho}\left(u-\frac{\nu}{\rho_j}\right)\right]c_{j-1,m}^{(2n+1)}+\left[1-\frac{2k\nu}{(\Delta\rho)^2}\right]c_{j,m}^{(2n+1)}$$

$$+k\left[\frac{\nu}{(\Delta\rho)^2}-\frac{1}{2\Delta\rho}\left(u-\frac{\nu}{\rho_j}\right)\right]c_{j+1,m}^{(2n+1)}$$

$$=k\left[-\frac{1}{2\Delta\theta}\frac{v}{\rho_j}-\frac{\nu}{\rho_j^2(\Delta\theta)^2}\right]c_{j,m-1}^{(2n)}+\left[1+\frac{2k\nu}{\rho_j^2(\Delta\theta)^2}\right]c_{j,m}^{(2n)}$$

$$+k\left[\frac{1}{2\Delta\theta}\frac{v}{\rho_j}-\frac{\nu}{\rho_j^2(\Delta\theta)^2}\right]c_{j,m+1}^{(2n)} \qquad (5)$$

$$k\left[\frac{\nu}{\rho_j^2(\Delta\theta)^2}+\frac{1}{2\Delta\theta}\frac{v}{\rho_j}\right]c_{j,m-1}^{(2n+2)}+\left[1-\frac{2k\nu}{\rho_j^2(\Delta\theta)^2}\right]c_{j,m}^{(2n+2)}$$

$$+k\left[\frac{\nu}{\rho_j^2(\Delta\theta)^2}-\frac{1}{2\Delta\theta}\frac{v}{\rho_j}\right]c_{j,m+1}^{(2n+2)}$$

$$=k\left[-\frac{\nu}{(\Delta\rho)^2}-\frac{1}{2\Delta\rho}\left(u-\frac{\nu}{\rho_j}\right)\right]c_{j-1,m}^{(2n+1)}+\left[1+\frac{2k\nu}{(\Delta\rho)^2}\right]c_{j,m}^{(2n+1)} \qquad (6)$$

$$+k\left[\frac{-\nu}{(\Delta\rho)^2}+\frac{1}{2\Delta\rho}\left(u-\frac{\nu}{\rho_j}\right)\right]c_{j+1,m}^{(2n+1)}$$

where (j, m) denotes the point at which the ρ- and θ-coordinates are $j\Delta\rho$ and $m\Delta\theta$, respectively. The superscript n is the number of the iteration cycle, and κ is the so-called overrelaxation parameter whose value may be picked to optimize the rate of convergence of the scheme. The velocity components u and v in general depend on j and m.

Finite-difference forms of the boundary conditions are obtained from Eqs. (3a-d). It should be remarked that the numerical approach used in the solution requires that the lattice be of finite size. Therefore, finite-difference boundary conditions corresponding to the analytic forms (3a) and (3b) are written for $\rho = \bar{J}\Delta\rho$ (where $\bar{J} \equiv j_{max}$ is finite) instead of for $\rho = \infty$. Finite-difference boundary conditions analogous to Eqs. (3c) and (3d) are written for $j = 0$.

Solution of Eqs. (5) and (6) also necessitates prescribing conditions (i.e., symmetry conditions) along the rays $\theta = 0$ and $\theta = \pi$, corresponding to values of $m = 0$ and $m = m_{max} \equiv \bar{M}$, respectively, where $\bar{M}$ is some finite integer.

The solution of the finite-difference problem is accomplished using the double-sweep or Gaussian elimination method; a brief summary of it is included here for the sake of completeness. When Eq. (5) or Eq. (6) is written for each mesh point, the resulting matrix of equations is tridiagonal. This means that the first and the last equations, which incorporate the boundary conditions, each contain only two unknowns. Therefore, beginning at the first row of the matrix, we can reduce the number of unknowns in every equation by one, and when the last row is reached the last equation becomes solved. Returning now from the last row back to the first completes the solution. For more detailed description of this method, the reader should refer to any standard text on numerical methods, e.g., Ref. 5.

3. Velocity Field

The considerations presented in Appendix I and Appendix II apply rigorously only to constant velocity fields; in view of the conclusion, however, that the implicit scheme converges under all conditions when $\kappa < 0$,

it is quite natural to use the procedure also when the coefficients are variable.

In the present investigation we are interested in low Reynolds number flow ($2 \leq Re \leq 20$), which is described adequately by the Oseen equations.[6] Unfortunately, the solution of these equations for the case of a circular cylinder[2] is in the form of an infinite series which (although absolutely convergent) converges so slowly that it is impossible to use it in numerical work, even with the help of a large digital computer. Neither is there available, at present, any satisfactory numerical algorithm for the determination of low Reynolds number viscous flow around a cylinder; therefore, this difficulty had to be circumvented by performing the computations with five different velocity distributions:

(a) undisturbed free stream $(u = \cos\theta,\ v = -\sin\theta)$ (7)

(b) potential flow (inviscid) described by

$$\left.\begin{aligned} u &= (1 - 1/\rho^2)\cos\theta \\ v &= -(1 + 1/\rho^2)\sin\theta \end{aligned}\right\} \tag{8}$$

(c) approximate Oseen flow[6] described by

$$\left.\begin{aligned} u &= \left[1 + \frac{\ln\left(\frac{Re}{8}\rho\right) + \Gamma - 1}{\ln\left(\frac{8}{Re}\right) - \Gamma + \frac{1}{2}}\right]\cos\theta \\ v &= -\left[1 + \frac{\ln\left(\frac{Re}{8}\rho\right) + \Gamma}{\ln\left(\frac{8}{Re}\right) - \Gamma + \frac{1}{2}}\right]\sin\theta \end{aligned}\right\} \tag{9}$$

where Γ = Euler's constant = 0.577... and the Reynolds number Re is defined by

$$Re \equiv U_\infty a/\bar{\nu}$$

in which $\bar{\nu}$ is the kinematic viscosity.

(d) approximate Oseen flow modified to satisfy the inviscid boundary condition exactly, i. e.,

$$\left.\begin{aligned} u &= \left[1 + \frac{\ln\left(\frac{Re}{8}\rho\right) + \Gamma - 1}{\ln\left(\frac{8}{Re}\right) - \Gamma + 1}\right]\cos\theta \\ v &= -\left[1 + \frac{\ln\left(\frac{Re}{8}\rho\right) + \Gamma}{\ln\left(\frac{8}{Re}\right) - \Gamma + \frac{1}{2}}\right]\sin\theta \end{aligned}\right\} \qquad (10)$$

(Note that neither approximation (c) nor (d) satisfies the viscous boundary condition $v\big|_{\rho=1} = 0$ except in the limit $Re \longrightarrow 0$.)

(e) quiescent fluid ($u \equiv 0$, $v \equiv 0$).

The intent here was to assess the influence of the velocity field; it is reasonable to expect that the correct solution lies somewhere in the region covered by the foregoing five cases. All of the above closed form expressions are easily programmed for use in conjunction with Eqs. (5) and (6); it would be equally convenient to store in the computer memory the numerical values of u and v if they were available.

III. RESULTS

1. General

In experiments being carried out at CAL,[7] typical free-stream conditions are on the order of $U_\infty = 500$ cm/sec , $p_t = 6$ mm Hg , $T = 300°K$, $c_\infty = 10^{-2}$; the gas is oxygen; $a = 0.2045$ cm , and $\theta_c = 159°$. For such conditions we have found it to be sufficient to use, in our computations, $\Delta\rho = 10^{-1}$, $\Delta\theta = \pi/20$, and to apply boundary conditions corresponding to (3a) and (3b) at $\rho = 6$ (i.e., $\bar{J} \equiv j_{max} = 60$, $\bar{M} \equiv m_{max} = 20$). For all iterations the initial guess was $c^{(0)} = 0$. For the dimensional coefficient of diffusion of O in O_2 we have used the relation $D = 233.7/p_t$, where p_t is the total pressure in mm Hg and D has the units cm^2/sec. This expression (cf. Ref. 8) may be expected to be a good approximation for all the experimental conditions considered here, in which the temperature does not deviate to any extent from 300°K.

Setting $\theta_c = \pi$ makes $c = c_\infty$ an exact solution of the problem and therefore enables us to check the convergence properties and accuracy of the scheme. Numerical experiments have shown that it is most efficient to use two values of κ : first, a large (absolute) value of about -1 forces the solution to approach its correct value rapidly but with sizable oscillations; then, when the oscillations are centered about the true solution, κ is decreased (in absolute value) to about -10^{-1} to damp them out. In order to speed up the convergence process further, the average value of two successive iterations is used as the initial guess for computation with the second, smaller, value of κ . The results of a typical trial computation are illustrated in Fig. 2. About 30 iterations are required to reduce the error to less than 0.1% everywhere in the mesh; to achieve this, the time required is about 10^{-2} hours on the IBM 7044.

Figure 3 represents a typical concentration field for a potential-flow velocity distribution; the wake-like effect at small θ is clearly discernible. For the sake of neatness, this result is presented for $\theta_c = 0$ (otherwise the curves cross).

From a series of plots like Fig. 3 for different values of γ we obtain the required relationship between the surface concentration $c_o(\theta)$ and γ ; a typical result is presented in Fig. 4.

This would be sufficient to use in conjunction with Eq. (1) to obtain the desired relationship between $\dot{q}$ and γ if it were not for the fact that $c_o(\theta)$ is a strong function of θ ; Fig. 5 represents typical distributions of concentration $c_o(\theta)$ along the surfaces of fully-catalytic and partially-catalytic cylinders. The catalytic heat transfer gauge employed in the experiments subtends an arc of 42° (21° on either side of the axis of symmetry, $\theta = \pi$) and, therefore, it is not reasonable to use any particular point value of c_o ; instead, in our computations we have employed the arithmetic mean of the two concentrations $c_o(\pi)$ and $c_o(\theta_c)$.

The computed results presented in Fig. 5 show a monotonic decrease in c_o towards the rear of the fully-catalytic cylinder. This finding agrees with the drop in local heat transfer with distance downstream from the front stagnation point of fully-catalytic cylinders observed by Myerson in recent CAL experiments. On the other hand, for the case where the catalytic surface extends only part way beyond the front stagnation point, the computations show a rapid rise in local surface concentration in the vicinity of the edge of the catalytic surface, with c_o ultimately approaching a value close to c_∞ . The part of the rise in c_o which takes place on the catalytic surface is attributable to diffusion of atoms from the outer and downstream part of the flow. For the case at hand (diffusion Reynolds number = 3.6), the effect on c_o of the cutoff in catalycity is noticeable all the way to the front stagnation point.

2. Prediction of the γ - $\dot{q}$ Relation for Test Conditions

The overall result of the computations, giving $\dot{q}$ as a function of γ , is shown in Fig. 6. (For convenience, Eq. (1) is incorporated into the program so that it is not necessary to examine the intermediate steps represented by Figs. 4 and 5; the machine output consists of the final Fig. 6 in tabular form.) The curves of Fig. 6 were computed for the two cases $c_o = \frac{1}{2}\left[c_o(\pi) + c_o(\theta_c)\right]$ (solid line) and $c_o = c_o(\pi)$ (dashed line);

in each case a potential velocity distribution was employed. The values of a , U_∞ , κ_∞ , T , p_t , and θ_c which were used are listed on the graph; these values correspond with values in CAL experiments currently being conducted. Thus, these results constitute a relationship predicted to exist under the specific test conditions, assuming that the convective flow is adequately represented by the postulated potential velocity field.

In order to estimate the effects of different velocity fields, Fig. 7 was prepared, for which the computations were carried out with $U_\infty = 150$ cm/sec and $\theta_c = 0$. The relatively small value of U_∞ was used because the approximate expressions for viscous flow description are considerably more accurate at lower Reynolds numbers. From Fig. 7 we see that the effect of the velocity distribution on the calculated heat transfer may be as much as 50%, although with reasonable approximate velocity distributions it is unlikely to exceed 20%; this conclusion agrees well with the same estimate arrived at analytically by Hartunian and his coworkers.[9] The different velocity fields used in the preparation of Fig. 7 are those listed in Sec. II-3.

Additional computations of this type with a higher free-stream velocity of $U_\infty = 593$ cm/sec presented in Fig. 8 reveal that the sensitivity of the computed heat transfer to the type of velocity distribution used in the computation increases rapidly with increasing free-stream velocity (cf. Fig. 7). It is also seen that at the stated free-stream velocity of 593 cm/sec, the heat transfer is about the same for potential flow and modified Oseen flow, which have different velocity fields, but which satisfy the same inviscid boundary condition $u = 0$.

Attempts to use results presented in Figs. 6, 7 and 8 disclose the fact that in the range of interest, $0.1 \leq \gamma \leq 0.2$, the curves have shallow slopes, which means that a small error in the determination of the heat transfer $\dot{q}$ leads to a large error in γ . (These curves are ideally suited for the inverse problem; i. e., for a given γ determine the heat transfer $\dot{q}$.) The shallowness of the slopes also implies that for a given $\dot{q}$, the corresponding computed value of γ is very sensitive to

the velocity distribution. In order to determine more favorable conditions, we have performed calculations for different free-stream concentration α_∞ , velocity U_∞ , and pressure p_t .

The top two curves in Fig. 8 illustrate the change obtained by increasing α_∞ to 3.5×10^{-2} and U_∞ to 5930 cm/sec. We see that the increase in the free-stream concentration translates the relevant curve upward without noticeably affecting its slope, a result which is expected because of the linearity of the problem. A tenfold increase in the free-stream velocity produces noticeable but still small increase in the slope.

Figure 9 shows curves which are very favorable for the purposes of this paper and for experiments: both the magnitude of the heat transfer and the slopes of the $\dot{q}$ vs. γ curves are large, leading to relatively greater accuracy in experimental measurements of $\dot{q}$, as well as higher certainty in the determination of γ . These curves are obtained by using not only high free-stream velocity and concentration, but also a very low pressure, as indicated on the figure. These conditions correspond to experiments and the supporting analysis reported by Hartunian and coworkers;[9] the solid curve in Fig. 9 corresponds to their apparatus, which consists of a fully-catalytic cylinder, and the dotted line is the corresponding result when only the heat transfer gauge is overlaid with catalytic material and the remaining cylinder surface is noncatalytic. The difference is seen to be very slight.

Hartunian's analysis is devised so as to yield not only the catalytic efficiency γ, but also the effective binary diffusion coefficient D which, in general, is found to differ from the value used in our work that we consider to be well established (see Refs. 8 and 10). Therefore, a direct comparison between the results of Hartunian et al. and our present findings is not possible; nevertheless, in spite of this and other uncertainties, the actual values of γ obtained agree reasonably well.

In summary, thus, the computations indicate that experiments of the type considered in this paper with the configuration as shown in Fig. 1, should be performed at as low a pressure and with as high a free-stream velocity as other constraints will allow.

3. Concluding Remarks

It has been demonstrated that the double sweep, alternating direction, implicit iteration procedure is a very efficient and powerful method for solving the convective diffusion equation with arbitrary boundary conditions. The program can be coupled easily to the necessary physico-chemical calculations to establish the relationship between the heat transfer and catalytic efficiency of the surface. The computations have disclosed that the result is sensitive to the velocity distribution, especially at Reynolds numbers higher than 3 or 4. Thus, further work on this problem, employing more realistic velocity distributions, is required.

A second possible refinement of the present work is the inclusion of a linear or quadratic source term in the convective diffusion equation to represent electron depletion or the two-body gas phase recombination processes, respectively. In view of the remarkable power of the finite difference scheme employed here, it is reasonable to expect that it will continue to work satisfactorily for those cases also. This expectation is supported by results of a recent theoretical investigation dealing with the application of the alternating-direction method to the diffusion equation with a source term.[11] Although convection was not included in the analysis of Ref. 11, the results of that work, together with the findings of our present study, suggest that the application of the alternating-direction scheme to the problem of convective diffusion with a source may be successfully carried out without much difficulty.

The natural extension of the work described in this paper would be application to three-dimensional problems such as, for example, the diffusion of electrons in the plasma sheath surrounding the Apollo vehicle reentering the atmosphere at an angle of attack. Present-day computers do not have sufficiently large memory capacity to handle this problem; however, such big computers will become available within the next year and, therefore, three-dimensional diffusion problems have been receiving considerable attention in the recent literature.[12]

A problem which is very well suited to the application of the method presented here, as well as being of interest from an experimental viewpoint, is the case of viscous laminar plane flow over a flat plate

(with a portion of the plate surface catalytically active). The chief advantage of this configuration is that the velocity components are known accurately and can be readily expressed numerically, in contrast to the case of flow past a cylinder. Furthermore, a Cartesian finite-difference mesh rather than a polar grid is appropriate to the flat-plate problem, and this lends itself to a more satisfactory prescription of boundary conditions remote from the surface. Experimentally, the flat-plate configuration should offer no disadvantage compared with the cylinder. For these reasons, it is felt that this problem is a very appropriate one for investigation.

REFERENCES

1. Rosner, D. E.: "Convective Diffusion as an Intruder in Kinetic Studies of Surface Catalyzed Reactions," AIAA Journal 2, pp. 593-610 (1964).
2. Faxén, H.: "Exacte Lösung der Oseenschen Differentialgleichungen einer Zähen Flüssigkeit fur den Fall der Translationsbewegung eines Zylinders," Nova Acta Regiae Soc. Scientiarum Upsaliensis, Vol. Ex. Ord. Ed. 1927, pp. 1-56 (Uppsala, 1927).
3. Prok, G. M.: "Effect of Surface Preparation and Gas Flow on Nitrogen Atom Surface Recombination," NASA TN D-1090 (1961).
4. Peaceman, D. W. and Rachford, H. H., Jr.: "The Numerical Solution of Parabolic and Elliptic Differential Equations," J. Soc. Indust. Appl. Math. 3, 1, pp. 28-41 (1955).
5. Richtmyer, R. D.: "Difference Methods for Initial-Value Problems," Interscience Publ. Inc., New York, pp. 101-104 (1964).
6. "Laminar Boundary Layers," (Ed. by L. Rosenhead), The Clarendon Press, Oxford, pp. 175, 190-192 (1963).
7. Myerson, A. L.: "Mechanisms of Surface Recombination from Step-Function Flows of Atomic Oxygen over Noble Metals," J. Chem. Phys. 42, 9, pp. 3270-3276 (1965).
8. Brokaw, R. S.: "Alignment Charts for Transport Properties Viscosity, Thermal Conductivity, and Diffusion Coefficients for Nonpolar Gases and Gas Mixtures at Low Density," NASA TR R-81 (1961).
9. Hartunian, R. A., Thompson, W. P., and Saffron, S.: "Measurements of Catalytic Efficiency of Silver for Oxygen Atoms and the $O\text{-}O_2$ Diffusion Coefficient," J. Chem. Phys. 43, 11, pp. 4003-4006 (1965); Also Rept. No. TDR-469(5240-20)-6, Aerospace Corp., El Segundo, Calif., 8 March 1965 by Lloyd, J. R. and Hartunian, R. A.

REFERENCES (Cont)

10. Krongelb, S. and Strandberg, M. W. P.: "Use of Paramagnetic-Resonance Techniques in the Study of Atomic Oxygen Recombinations," J. Chem. Phys. 31, 5, pp. 1196-1210 (1959).

11. Albrecht, J.: "Eine Verallgemeinerung des Verfahrens der alternierenden Richtungen," Z. A. M. M. 45, Sonderheft, pp. T3-T6 (1965).

12. Fairweather, G. and Mitchell, A. R.: "A New Alternating Direction Method for Parabolic Equations in Three Space Variables," J. Soc. Indust. Appl. Math. 13, 4, pp. 957-965 (1965).

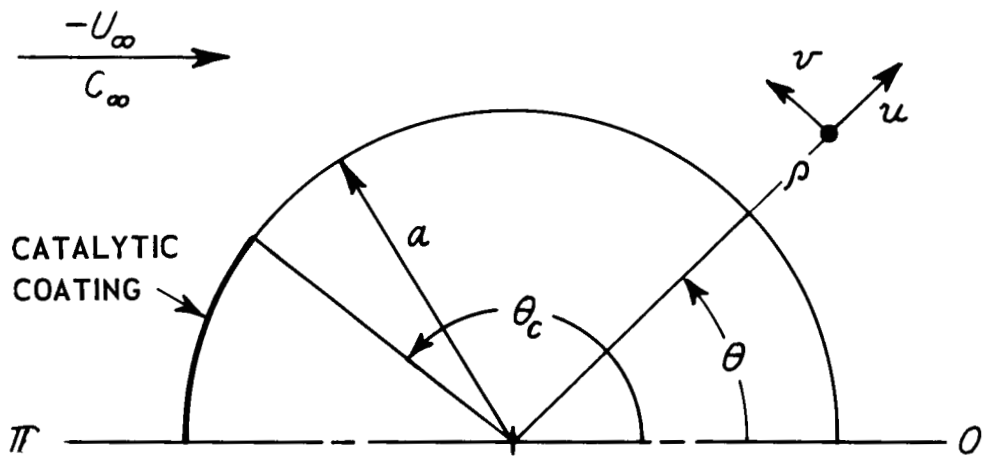

Figure 1 GEOMETRY AND COORDINATE SYSTEM

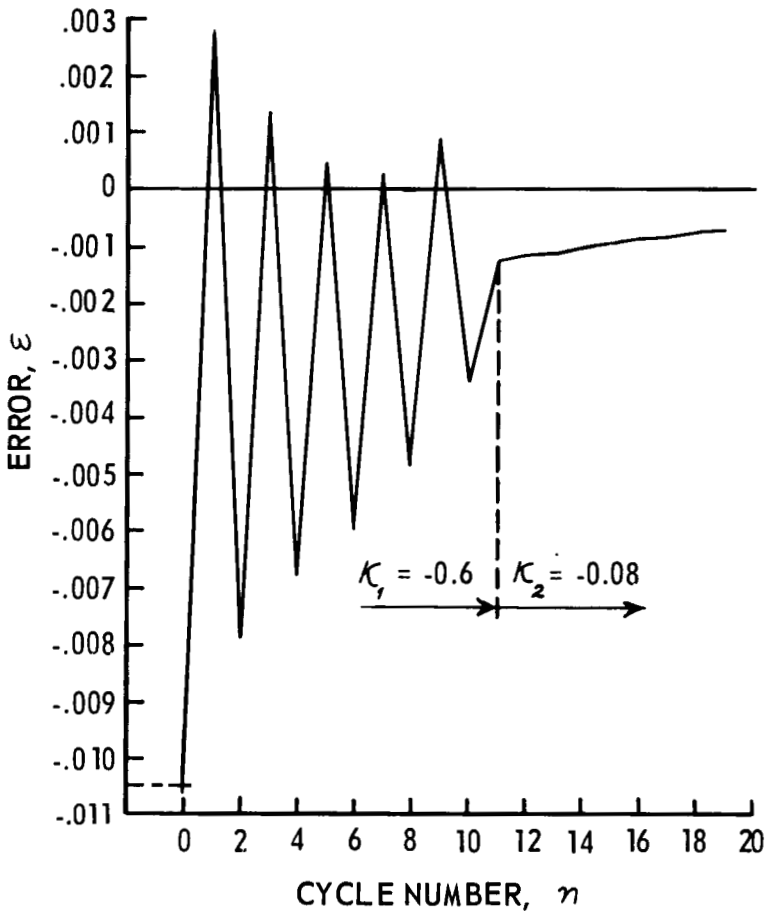

Figure 2 CONVERGENCE OF ITERATION SCHEME

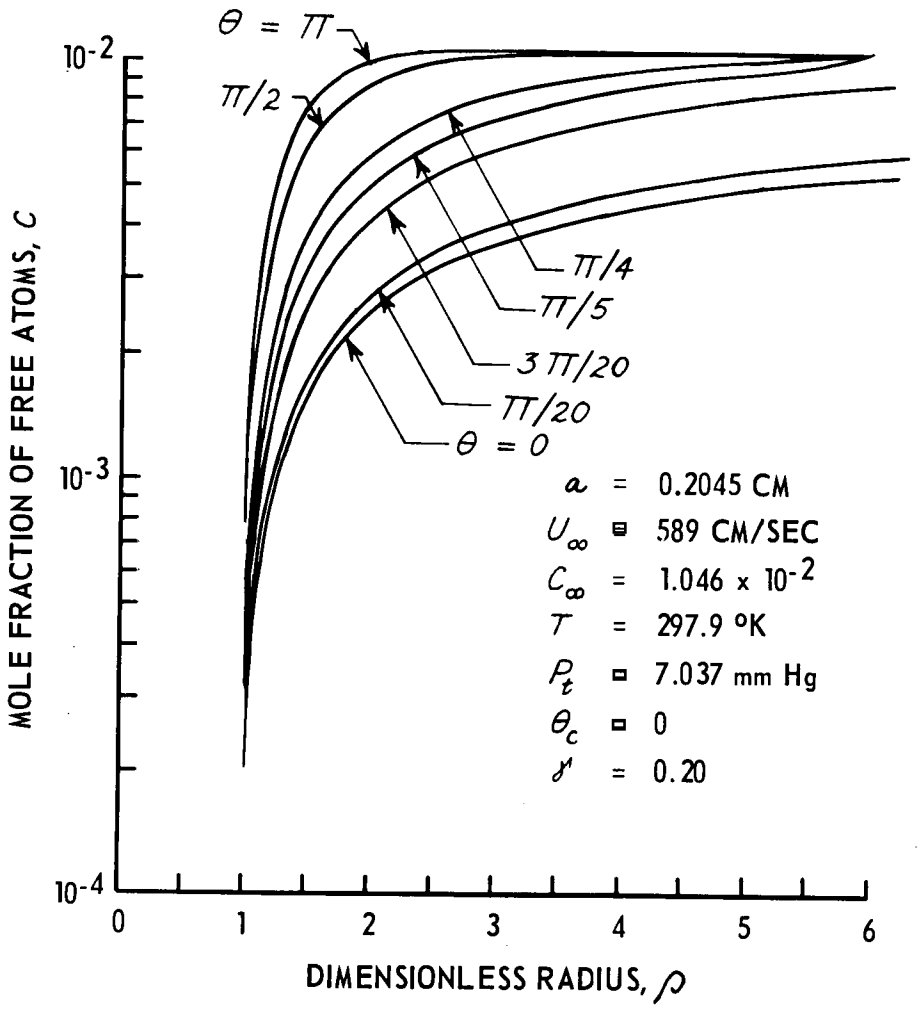

Figure 3 TYPICAL OXYGEN ATOM CONCENTRATION FIELD FOR POTENTIAL FLOW

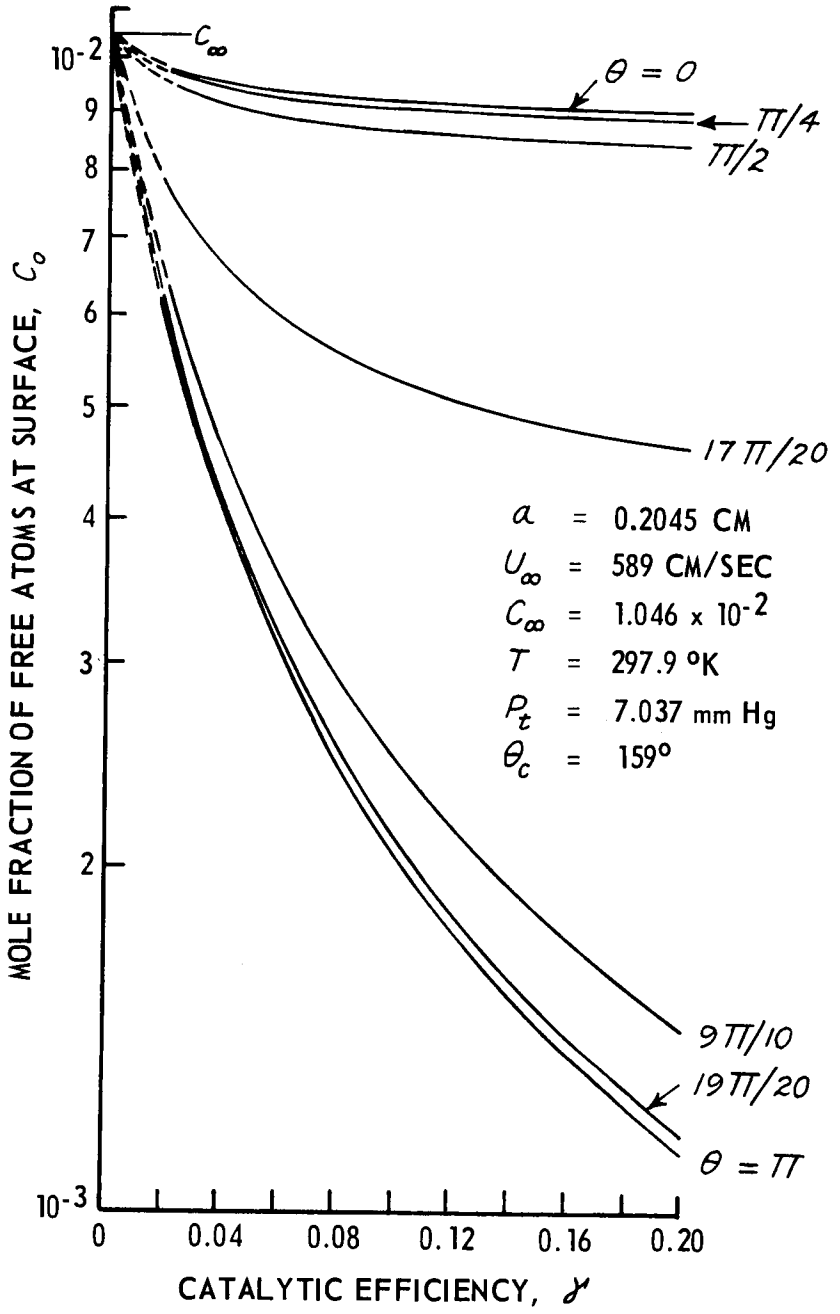

Figure 4 SURFACE CONCENTRATION OF FREE OXYGEN ATOMS VS. CATALYTIC EFFICIENCY OF SURFACE (POTENTIAL FLOW)

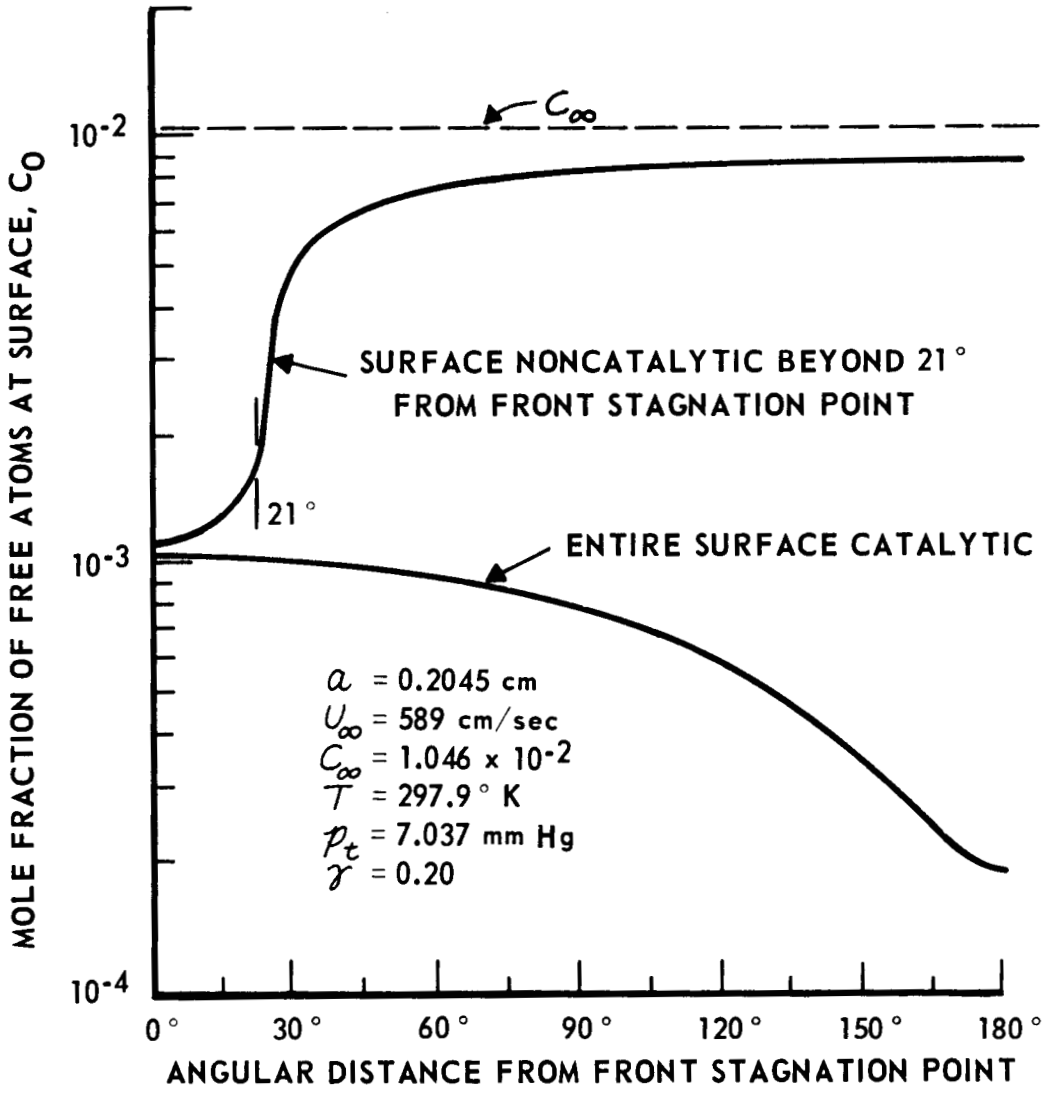

Figure 5 VARIATION OF FREE OXYGEN ATOM CONCENTRATION ALONG SURFACE OF CYLINDER IN POTENTIAL FLOW -- FULLY CATALYTIC AND PARTIALLY CATALYTIC SURFACES

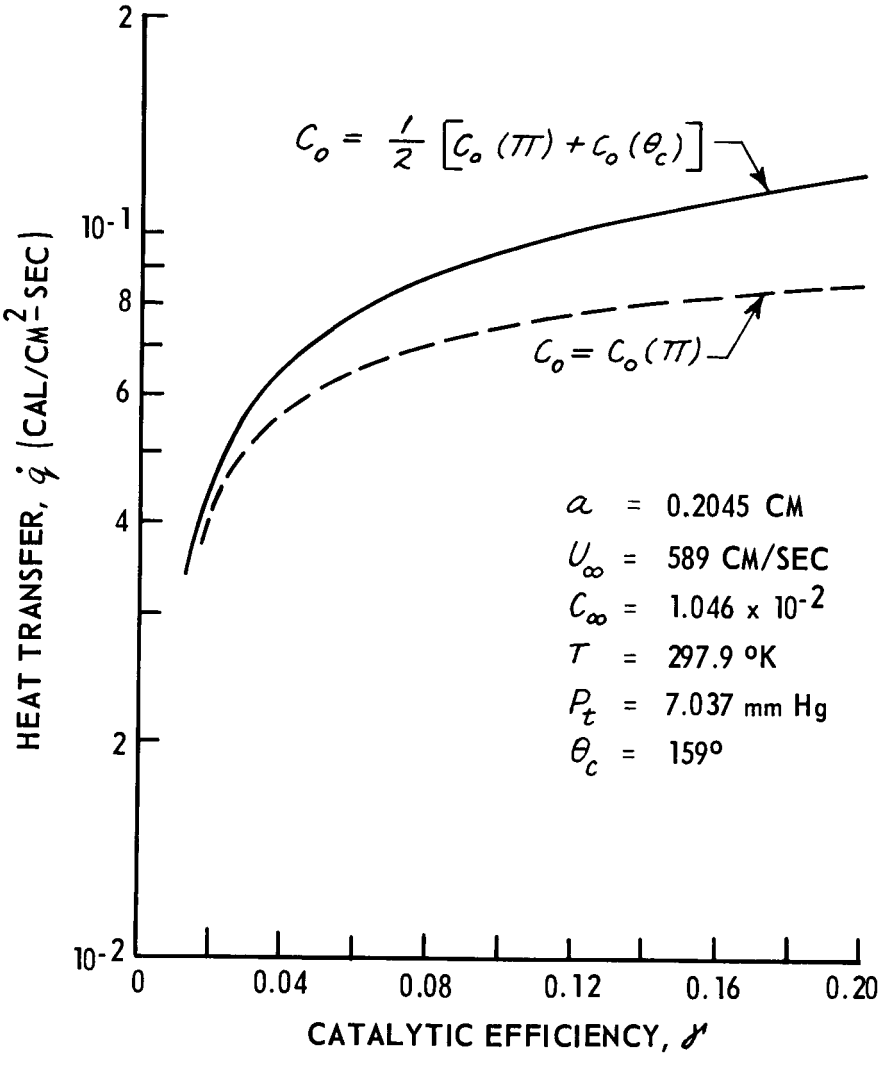

Figure 6 HEAT TRANSFER RATE VS. CATALYTIC EFFICIENCY FOR OXYGEN RECOMBINATION (POTENTIAL FLOW)

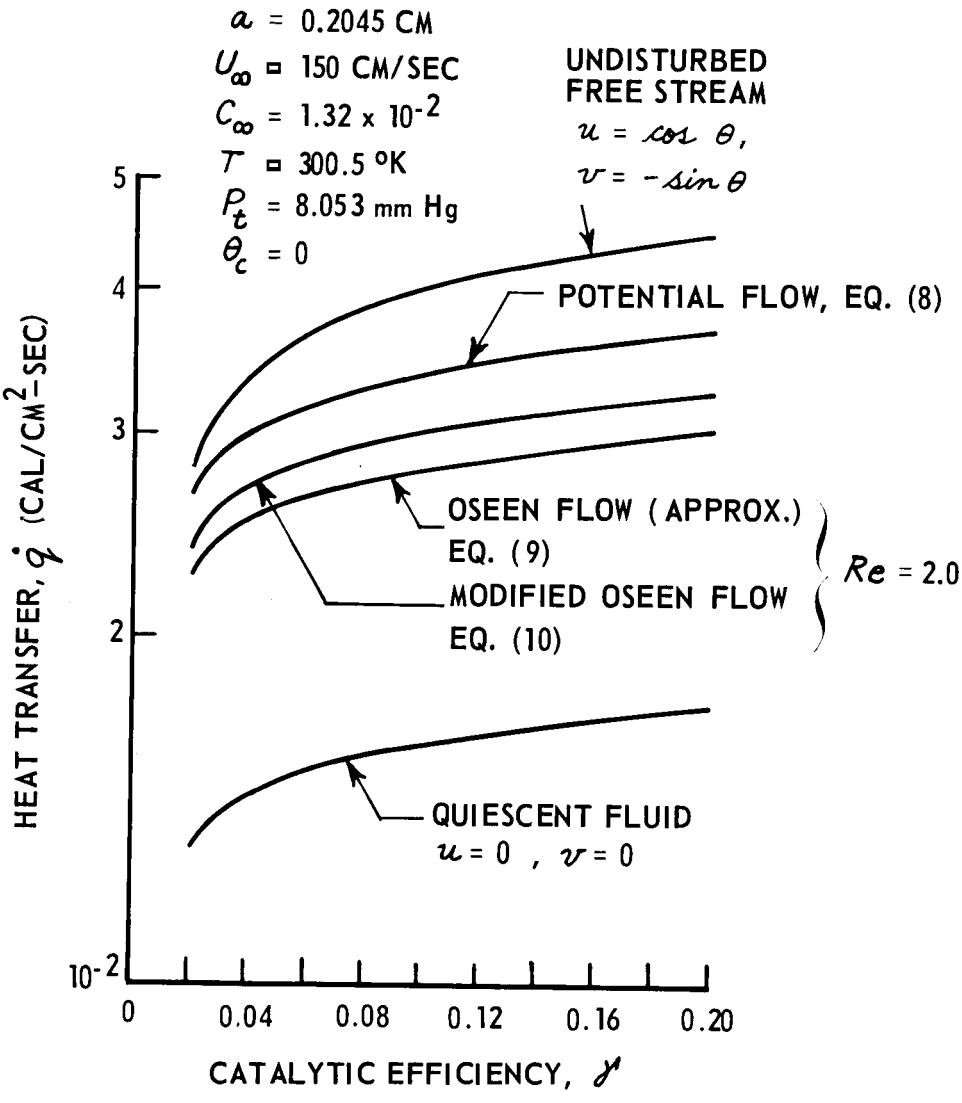

Figure 7 EFFECT OF VELOCITY FIELD ON THE γ'-$\dot{q}$ RELATIONSHIP FOR OXYGEN RECOMBINATION

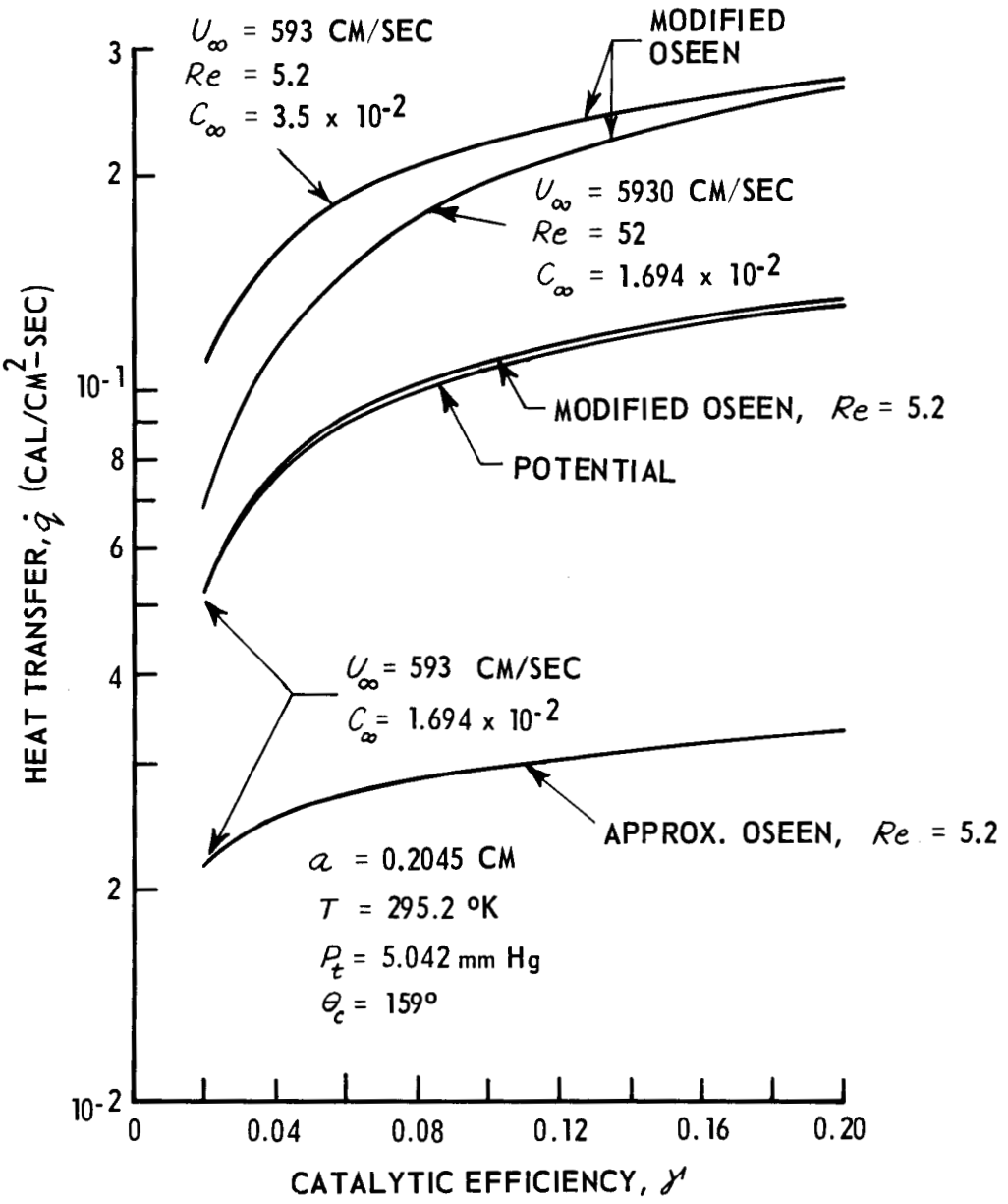

Figure 8 EFFECT OF FREE-STREAM CONCENTRATION, FREE-STREAM VELOCITY, AND VELOCITY FIELD ON THE $\gamma'-\dot{q}$ RELATIONSHIP FOR OXYGEN RECOMBINATION

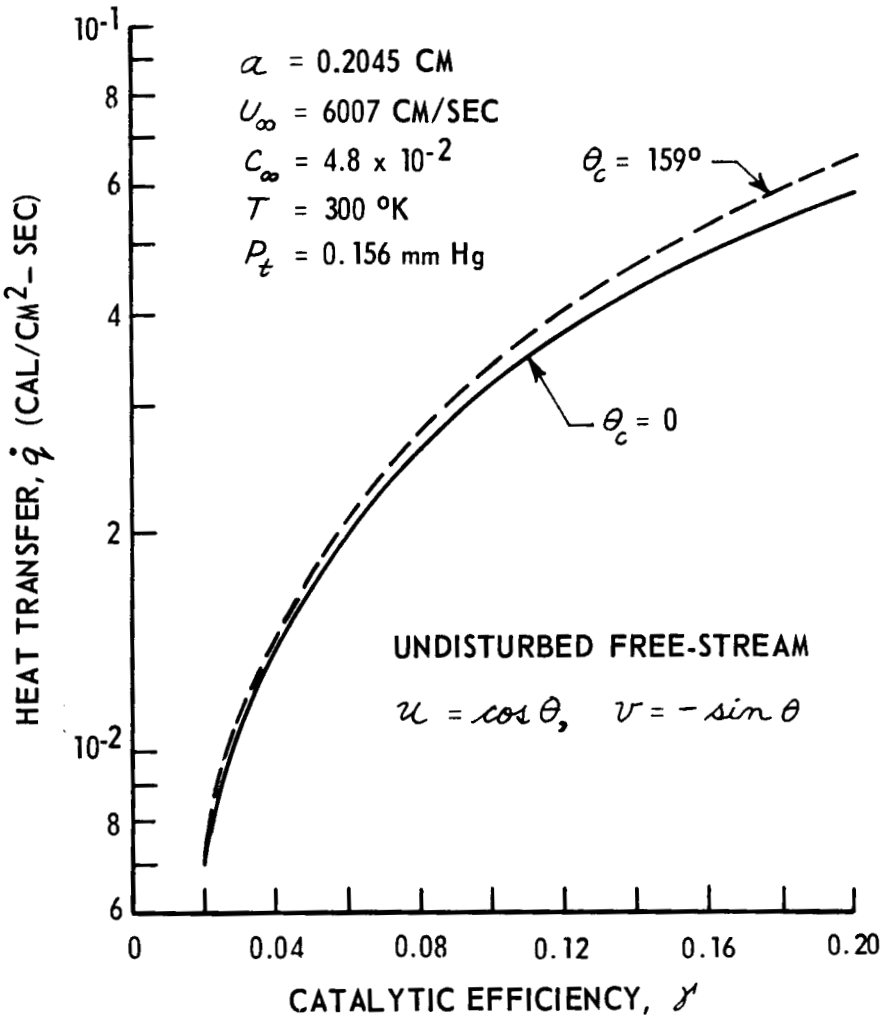

Figure 9 HEAT TRANSFER RATE VS. CATALYTIC EFFICIENCY FOR OXYGEN RECOMBINATION -- HIGH FREE-STREAM ATOM CONCENTRATION AND VELOCITY (EXPERIMENTAL CONDITIONS OF HARTUNIAN et. al.)

APPENDIX I

CONVERGENCE ANALYSIS -- EXPLICIT ITERATION SCHEME

In this first Appendix we shall describe an explicit iteration procedure and determine its limitations. For convenience, the discussion here and in Appendix II will be presented in the Cartesian coordinates.

With the notation

$$c_x = \frac{1}{\Delta x}\left[c(x+\Delta x) - c(x)\right]$$

$$c_{\bar{x}} = \frac{1}{\Delta x}\left[c(x) - c(x-\Delta x)\right]$$

$$c_{\hat{x}} = \frac{1}{2\Delta x}\left[c(x+\Delta x) - c(x-\Delta x)\right]$$

the finite-difference analog of Eq. (2) (in Cartesian coordinates) is:

$$u(j,m)\, c_{\hat{x}}(j,m) + v(j,m)\, c_{\hat{y}}(j,m) = \nu\left[c_{x\bar{x}}(j,m) + c_{y\bar{y}}(j,m)\right] \tag{AI-1}$$

where (j, m) denotes the point at which the x- and y-coordinates are $j\Delta x$ and $m\Delta y$, respectively.

An explicit iteration procedure for the determination of the function c which would satisfy (AI-1) can be represented as follows:

$$c^{(n+1)} = c^{(n)} - K R c^{(n)} \tag{AI-2}$$

where K is the relaxation parameter, the index n is the number of the iteration cycle, and R denotes the residue operator defined by

$$R_c = u c_{\hat{x}} + v c_{\hat{y}} - \nu(c_{x\bar{x}} + c_{y\bar{y}})$$

Clearly the condition for convergence is:

$$\left| R c^{(n+1)} \right| \leq \left| R c^{(n)} \right| \tag{AI-3}$$

In order to relate requirement (AI-3) to conditions on the mesh size, on κ and on ν we shall employ the von Neumann stability analysis.

Setting

$$c^{(n)}(x,y) = e^{i\alpha x}\, e^{i\beta y} \tag{AI-4}$$

and substituting into (AI-2) we obtain:

$$c^{(n+1)}(j,m) = (1 - \kappa F)\, c^{(n)}(j,m) \tag{AI-5}$$

where F calculated explicitly is:

$$\begin{aligned} F = {} & e^{i\alpha\Delta x}\left[\frac{u}{2\Delta x} - \frac{\nu}{(\Delta x)^2}\right] - e^{-i\alpha\Delta x}\left[\frac{u}{2\Delta x} + \frac{\nu}{(\Delta x)^2}\right] \\ & + e^{i\beta\Delta y}\left[\frac{v}{2\Delta y} - \frac{\nu}{(\Delta y)^2}\right] - e^{-i\beta\Delta y}\left[\frac{v}{2\Delta y} + \frac{\nu}{(\Delta y)^2}\right] \\ & + 2\left[\frac{\nu}{(\Delta x)^2} + \frac{\nu}{(\Delta y)^2}\right] \end{aligned} \tag{AI-6}$$

At this point we must, in order to make further progress, assume that F is independent of j and m, i.e., impose the restriction that u and v are constants. Then

$$Rc^{(n+1)} = (1 - \kappa F)\, Rc^{(n)}$$

and condition (AI-3) reduces to

$$\left| 1 - \kappa F \right| \leq 1 \tag{AI-7}$$

for all α and β.

Denoting the real part of F by $2\nu g$ and the imaginary part by h where

$$g = \frac{1}{(\Delta x)^2}\left[1 - \cos(\alpha\Delta x)\right] + \frac{1}{(\Delta y)^2}\left[1 - \cos(\beta\Delta y)\right]$$

and

$$h = -\left[\frac{u}{\Delta x}\sin(\alpha\Delta x) + \frac{v}{\Delta y}\sin(\beta\Delta y)\right]$$

requirement (AI-7) becomes:

$$0 \le \kappa \le 4\nu g/(4\nu^2 g^2 + h^2) \qquad \text{(AI-8)}$$

Now it is clear that the most favorable situation (the largest allowable value of κ) obtains for $u = v = 0\ (h \equiv 0)$ and that then (AI-8) reduces to:

$$0 \le \kappa \le \frac{1}{2\nu\left[\frac{1}{(\Delta x)^2} + \frac{1}{(\Delta y)^2}\right]} \qquad \text{(AI-9)}$$

It is known that such a small value of the relaxation parameter κ requires an excessively large number of iteration cycles before the initial guess is brought sufficiently close to the true solution. For example, if $\Delta x = \Delta y$, then from (AI-9)

$$0 \le \kappa\,(\Delta x)^2/4\nu \qquad \text{(AI-10)}$$

and since it is not uncommon for ν to be about 20 or 30 in physical applications (ν being the nondimensional diffusivity), each iteration cycle can reduce the error only by the factor $(\Delta x)^2/100$.

APPENDIX II

CONVERGENCE ANALYSIS -- IMPLICIT ITERATION SCHEME

The conclusion of Appendix I makes it necessary to use an implicit iteration procedure. From the results known for the Laplace equation,[4] the most natural scheme to try is the alternating-direction method.

For the finite-difference equation (AI-1), this algorithm is given by:

$$\left.\begin{aligned} c_{j,m}^{(2n+1)} &= c_{j,m}^{(2n)} + K\left[u\, c_{\hat{x}}^{(2n+1)} - \nu c_{x\bar{x}}^{(2n+1)} + v\, c_{\hat{y}}^{(2n)} - \nu c_{y\bar{y}}^{(2n)}\right] \\ c_{j,m}^{(2n+2)} &= c_{j,m}^{(2n+1)} + K\left[u\, c_{\hat{x}}^{(2n+1)} - \nu c_{x\bar{x}}^{(2n+1)} + v\, c_{\hat{y}}^{(2n+2)} - \nu c_{y\bar{y}}^{(2n+2)}\right] \end{aligned}\right\} \quad \text{(AII-1)}$$

For convenience, we introduce the following notation:

$$r = \frac{1}{2}u\Delta x - \nu$$

$$\ell = -\frac{1}{2}u\Delta x - \nu$$

$$t = \frac{1}{2}v\Delta y - \nu$$

$$b = -\frac{1}{2}v\Delta y - \nu$$

Since (AII-1) is linear, the error ε satisfies the same equation as c itself; with the above notation, the equations for the error are:

$$\left.\begin{aligned} \varepsilon_{j,m}^{(2n+1)} &= \varepsilon_{j,m}^{(2n)} + \frac{K}{(\Delta x)^2}\left[r\,\varepsilon_{j+1,m}^{(2n+1)} + 2\nu\varepsilon_{j,m}^{(2n+1)} + \ell\,\varepsilon_{j-1,m}^{(2n+1)}\right] \\ &\quad + \frac{K}{(\Delta y)^2}\left[t\,\varepsilon_{j,m+1}^{(2n)} + 2\nu\varepsilon_{j,m}^{(2n)} + b\,\varepsilon_{j,m-1}^{(2n)}\right] \\ \varepsilon_{j,m}^{(2n+2)} &= \varepsilon_{j,m}^{(2n+1)} + \frac{K}{(\Delta x)^2}\left[r\,\varepsilon_{j+1,m}^{(2n+1)} + 2\nu\varepsilon_{j,m}^{(2n+1)} + \ell\,\varepsilon_{j-1,m}^{(2n+1)}\right] \\ &\quad + \frac{K}{(\Delta y)^2}\left[t\,\varepsilon_{j,m+1}^{(2n+2)} + 2\nu\varepsilon_{j,m}^{(2n+2)} + b\,\varepsilon_{j,m-1}^{(2n+2)}\right] \end{aligned}\right\} \quad \text{(AII-2)}$$

Assuming the error to be of the form

$$\varepsilon_{j,m}^{(n)} = e^{i\alpha x} e^{i\beta y} e^{\gamma n} \tag{AII-3}$$

and substituting it into (AII-2) we obtain

$$\varepsilon_{j,m}^{(2n+1)} \left[1 - \frac{K}{(\Delta x)^2} A\right] = \varepsilon_{j,m}^{(2n)} \left[1 + \frac{K}{(\Delta x)^2} B\right]$$

$$\varepsilon_{j,m}^{(2n+2)} \left[1 - \frac{K}{(\Delta y)^2} B\right] = \varepsilon_{j,m}^{(2n+1)} \left[1 + \frac{K}{(\Delta x)^2} A\right] \tag{AII-4}$$

where

$$A = r e^{i\alpha\Delta x} + 2\nu + \ell e^{-i\alpha\Delta x}$$

$$B = t e^{i\beta\Delta y} + 2\nu + b e^{-i\beta\Delta y}$$

Relevant to stability is the error growth in one cycle, that is, in two sweeps of the mesh (one in each direction). The stability condition is, therefore

$$\left| \frac{\varepsilon_{j,m}^{(2n+2)}}{\varepsilon_{j,m}^{(2n)}} \right| \leq 1 \tag{AII-5}$$

Using (AII-4) in (AII-5) we obtain

$$\left| \frac{1 + K A/(\Delta x)^2}{1 - K A/(\Delta x)^2} \right| \left| \frac{1 + K B/(\Delta y)^2}{1 - K B/(\Delta y)^2} \right| \leq 1 \tag{AII-6}$$

A sufficient condition for the above inequality to hold is that each factor be less than unity.

Since the linear fractional transformation

$$\zeta = \frac{1+z}{1-z}$$

maps (conformally) the left half-plane onto the unit disc and A and B are complex numbers, (AII-6) will be satisfied if $Re\left\{\kappa A/(\Delta x)^2\right\} \leq 0$ and $Re\left\{\kappa B/(\Delta y)^2\right\} \leq 0$.

Substituting here the definitions of A, B, r , ℓ , t , and b, we find that the scheme is stable for all mesh sizes if $\kappa < 0$.